12^{th} International Conference on Fracture Mechanics of Concrete and Concrete Structures
FraMCoS-12
B.L.A. Pichler, Ch. Hellmich, P. Preinstorfer (Eds)

https://doi.org/10.21012/FC12.1198
MS04:5

MODELING TOUGHENING MECHANISMS IN CONCRETE USING MULTISCALE PHASE FIELD APPROACH

Anupama Surendran[†*], **J M Chandra Kishen**[†‡]

[†] Indian Institute of Science, India

[*] e-mail: anupamas@iisc.ac.in

[‡]e-mail: chandrak@iisc.ac.in

Key words: Phase-field, Meso-scale, Interface fracture

Abstract. Understanding crack propagation in concrete across different length scales is essential for capturing the intricate failure mechanisms that arise from its highly heterogeneous structure. However, fracture simulations in concrete often have significant computational costs and implementation difficulties. Phase-field models address these challenges by capturing crack phenomena, such as nucleation and propagation while maintaining easiness in implementation. Despite the advantages of phase-field models, their application to fracture analysis of concrete at multiple length scales is limited. Existing phase field models often face substantial computational costs while accounting for material heterogeneity. To address these challenges, a multiscale phase-field fracture study is presented in this work. The focus of the study is to model heterogeneity while maintaining computational efficiency. The first part of this work focuses on generating the meso-scale structure of concrete. This includes considering meso-scale features such as aggregate volume fraction, the interfacial transition zone, and air voids. The second part addresses formulating the multiscale phase-field fracture problem. A three-point bending test is conducted to investigate the fracture phenomena in detail. meso-scale crack toughening mechanisms, such as aggregate bridging and crack deflection, were observed in the model. The fracture energy and tensile strength values are investigated in detail. Finally, the accuracy of the presented model is evaluated by comparing the load-displacement data with experimental results. The findings of this study provide valuable insights for developing more efficient and scalable phase field modelling approaches for fracture phenomena in concrete.

1 INTRODUCTION

Concrete is an extensively used engineering material with very complex material behavior. Its highly heterogeneous microstructure, composed of aggregates, cement paste, and the interfacial transition zone (ITZ), makes the study of crack propagation and failure particularly challenging. Unique crack propagation mechanisms, such as crack deflection, crack arrest, and aggregate bridging, emerge from the interactions between these different constituents. While experimental efforts are time-consuming and costly, computational models face challenges in accounting for heterogeneity due to their extremely high computational costs.

The introduction of phase-field fracture models has significantly improved fracture simulations by offering a reliable framework that is easy to implement [1–3]. Although the phase-field model is straightforward for simulating brittle fracture, it requires additional consideration when applied to quasi-brittle materials like concrete. In this regard, several robust macroscopic models have been developed that are ca-

pable of predicting concrete fracture with considerable accuracy [4–6]. For instance, Wu et al. [6] proposed a macroscopic uniform phase-field theory for quasi-brittle materials by making use of the cohesive zone model, enhancing the model's ability to capture concrete fracture. However, macroscopic models do not account for the individual effects of aggregates, mortar, and the interfacial transition zone (ITZ); instead, they consider a homogenized response for the material as a whole. A mesoscopic model is essential to obtain a clear understanding of the crack propagation mechanisms and the influence of each constituent on concrete failure. Nonetheless, challenges persist in generating highly heterogeneous mesostructures of concrete, modeling the ITZ, and managing a large number of degrees of freedom along with the corresponding computational costs. As a result, meso-scale fracture models for concrete remain limited.

In this study, we simulate fracture in concrete using a multi-phase phase-field model. A meso-scale simulation, incorporating aggregates, mortar, and ITZ, is conducted in the crack propagation regime, while a macroscopic model is applied in other regions of the material behavior. The phase field model is used to represent the crack and ITZ. Various crack propagation mechanisms, such as aggregate bridging and crack deflection are observed in the model, providing valuable insights into the fracture process. Additionally, the influence of the mesostructure on the fracture behavior of concrete is also examined.

2 METHODOLOGY

The details of the mesostructure generation, phase field model, interface model and post-processing calculations used in this work are outlined in this section.

2.1 Mesostructure generation

In this model, aggregates are idealized as circular shapes. The size and distribution of the aggregates are randomly generated based on a specified aggregate volume fraction. A representative volume element (RVE) is considered in the crack propagation regime for mesostructure generation. The process of mesostructure generation is depicted in a flowchart shown in Figure 1. Figure 2 shows the schematic representation of a three-point bending specimen, and Figure 3 shows the generated mesostructure inside the RVE.

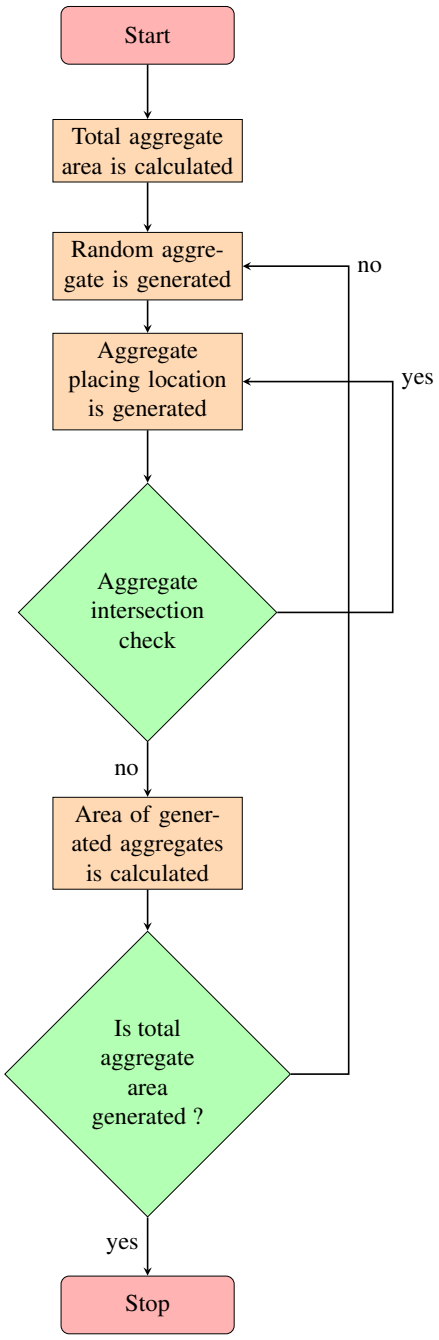

Figure 1: Mesostructure generation procedure

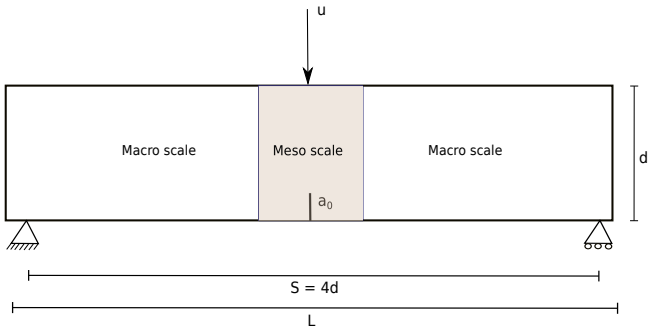

Figure 2: Schematic diagram of the three-point bending test specimen

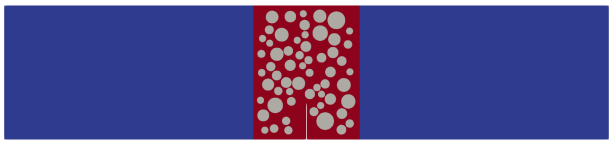

Figure 3: Mesostructure generated in three-point bending specimen

2.2 Phase-field fracture model

Phase-field models are employed to model moving interface problems related to irreversible processes. The foundation of phase-field fracture models is based on Griffith's theory of brittle fracture [7]. The energy minimization problem introduced by [7] is further developed into a variational formulation based on the energy functional [8]. The energy functional associated with a solid in domain Ω containing a crack Γ is given by,

$$E(u,\Gamma) = \int_{\Omega} \Psi(\varepsilon(u))dx + G_c \int_{\Gamma} ds \qquad (1)$$

where u is the displacement field, Γ is the admissible crack set, ε is the elastic strain, G_c is the material fracture toughness, Ψ is the elastic energy density. A regularized energy functional is used to alleviate the numerical difficulty [9] in phase-field models. The regularized energy functional is given by,

$$E_l(u,\phi) = \int_{\Omega} g(\phi)\Psi(\varepsilon(u))dx + G_c \int_{\Omega} \gamma_l(\phi,\nabla\phi)dx \qquad (2)$$

where, ϕ is a scalar variable called the phase field and represent the damage state of the system, $g(\phi)$ is called a degradation function and is given by,

$$g(\phi) = (1-\phi)^2 + \eta \qquad (3)$$

γ_l is a second order function used for regularization given by,

$$\gamma_l(\phi,\nabla\phi) = \frac{1}{2l}(\phi^2 + l^2|\nabla\phi|^2) \qquad (4)$$

l is a modelling parameter called length scale parameter.

The interface is represented by using a static phase field variable β which is obtained from solving a phase field problem [10] in the solid domain given by,

$$\begin{aligned} \beta(x) - l_{int}^2 \Delta\beta(x) &= 0 \text{ in } \Omega \\ \beta(x) &= 1 \text{ on } \Gamma_i \\ \nabla\beta(x) &= 0 \text{ on } \partial\Omega \end{aligned} \qquad (5)$$

where, Γ_i is the interface between two material and l_{int} is the interface length scale parameter . β = 1 across the points on the interface and β = 0 in the points far away from interface. The interface phase field problem solved across the domain illustrated in Figure 2 is shown in Figure 4.

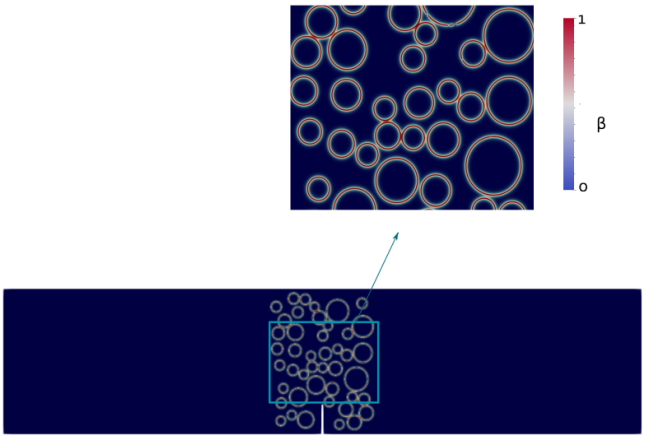

Figure 4: Interface phase field variable β

After obtaining interface phase field parameter an interface fracture toughness value of G_c^{int} is assigned across the interface and an interface fracture energy term is added to the energy functional [11]. Energy functional for the problem containing both crack and interface in the domain is given by,

$$E(u,\phi,\beta) = \int_\Omega \Psi(\varepsilon(u),\phi) + \int \phi^2 G_i \gamma(\beta,\nabla\beta) + \int (1-\beta) G_c \gamma(\phi,\nabla\phi) \quad (6)$$

where, the terms are corresponding to strain energy, interface fracture energy and bulk fracture energy respectively. The phase field problem is solved by solving Equation 6 using the finite element method.

3 Results and discussions

A three-point bending test is conducted on the beam depicted in Figure 2. The dimensions of the beam and the material properties employed in the simulations are provided in Table 1 and 2, respectively.

Table 1: Geometry of the specimen

	L (mm)	D (mm)	a_0 (mm)
Beam dimensions	340	75	15

Four samples, each with randomly generated mesostructures, are utilized in the simulation. The macroscale crack propagation path for the specimen is shown in Figure 5. The load-displacement data is obtained at the load application point for all four samples and is plotted in Figure 6. It can be observed that the peak load varies among the four specimens, despite having the same aggregate volume fraction, suggesting a strong dependence of material behavior on the mesostructure. Different mesostructures exhibit variations in aggregate shape and the spatial distribution of aggregates. Additionally, each mesostructure may have a distinct volume fraction of the interfacial transition zone.

Table 2: Material properties

	Young's modulus (GPa)	Poisson's ratio	Fracture energy (N/mm)
Concrete	35.30	0.20	0.12
Aggregate	55.00	0.20	-
Mortar	20.00	0.20	0.11

To gain further insights, the effective fracture energy (G_{eff}) is quantified for three different samples.

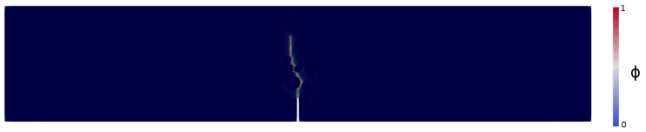

Figure 5: Final crack propagation path

G_{eff} is calculated as the rate of total fracture energy E_{frac} with respect to crack length a.

$$G_{eff} = \frac{\partial E_{frac}}{\partial a} \quad (7)$$

where the total fracture energy, obtained by adding the bulk fracture energy and interface fracture energy.

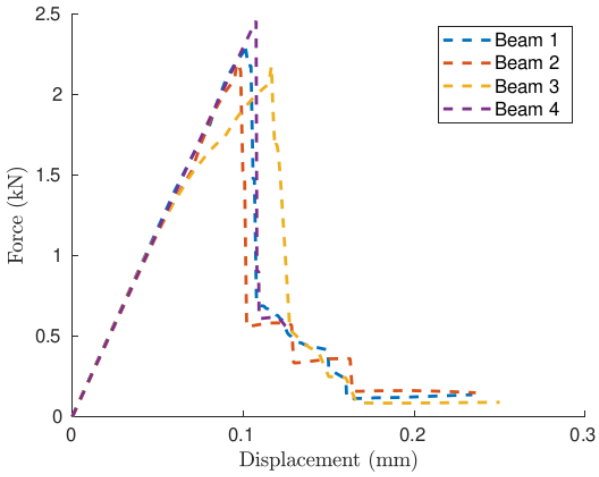

Figure 6: Load displacement diagram for different mesostructures

The effective fracture energy for the three different samples, as shown in Figure 7, is plotted in Figure 8. The meso-scale crack propagation figures clearly illustrate various crack toughening mechanisms, such as crack arrest, aggregate bridging, and crack deflection. As the crack begins to propagate, it deviates from its path in all three samples due to the presence of aggregates. However, in sample 3, the crack is arrested before it can propagate further. This is evident in Figure 8, where the effective fracture energy (G_{eff}) shows a significant increase compared to samples 1 and 2. However, once the specimen reaches the stage of complete damage (i.e., when the crack length exceeds 40 mm), the effective fracture energy converges to 0.12, which corresponds to the critical fracture energy (G_c) of concrete.

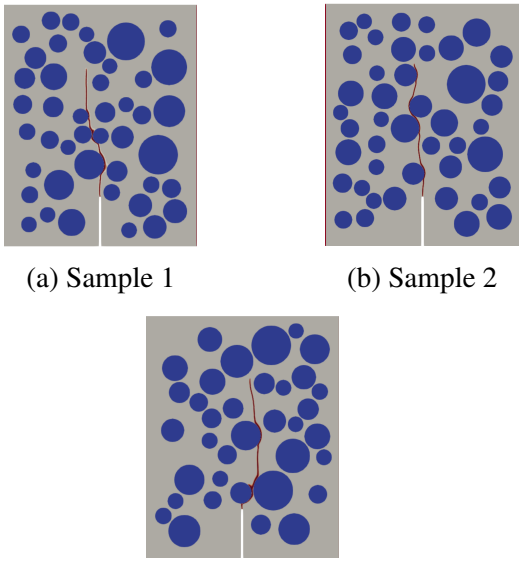

(a) Sample 1 (b) Sample 2

(c) Sample 3

Figure 7: Crack propagation path associated with different mesostructures

The material response of the three samples shown in Figure 7 is characterized using peak load and effective fracture energy (G_{eff}) at failure. These results are summarized in Table 4. As seen in Table 4, the peak load shows a greater degree of variation compared to the effective fracture energy. The load-displacement diagram obtained from the phase-field simulation is also compared with the experimental results presented by Keerthana et al. [12], as shown in Figure 9. An important observation from Figure 9 is that the area under the load-displacement curve in the experimental results is larger than that in the numerical simulation. This suggests that the softening behavior observed in the experimental data is more pronounced compared to the numerical simulation, indicating a lower softening effect in the latter. However, this discrepancy can be attributed to the fact that only aggregates larger than 4.75 mm were considered, while the effects of micro-heterogeneities, such as smaller aggregates and air voids, were neglected. To achieve more accurate results, it is essential to include these micro-heterogeneities in the analysis.

Table 3: Material properties

	Peak load (kN)	G_{eff} (N/mm)
Sample 1	2.35	0.126
Sample 2	2.30	0.116
Sample 3	2.71	0.134

Table 4: Peak load and fracture energies of specimen

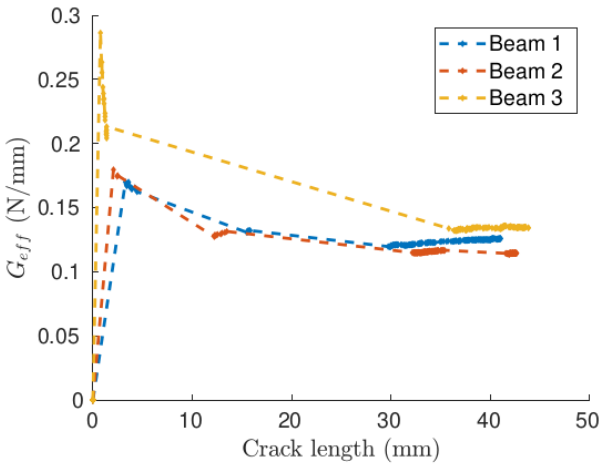

Figure 8: Effective fracture energies of the specimen

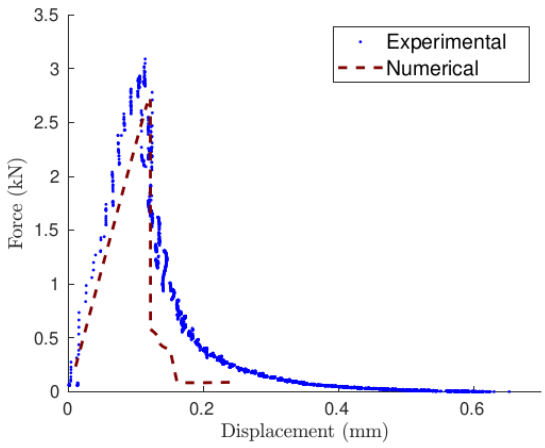

Figure 9: Load displacement diagram: comparison with experimental data

4 Conclusions

A multiscale phase field study is carried out to investigate the fracture behaviour of concrete. Meso-scale analysis is performed in the crack propagation regime, while macroscale analysis is applied in other regions. The model successfully captures crack propagation mechanisms, including aggregate bridging, crack deflection, and crack arrest. Comparisons between numerical simulations and experimental results reveal a lower softening effect in the numerical predictions. This can be attributed to the exclusion of micro-heterogeneities such as smaller aggregates and air voids. Future work will focus on incorporating these micro-heterogeneities to improve the model's accuracy. The findings offer valuable insights into the fracture behavior of concrete and the development of efficient computational models.

REFERENCES

[1] Francfort, G. A., and Marigo, J.-J. 1998. Revisiting brittle fracture as an energy minimization problem, *Journal of the Mechanics and Physics of Solids*, Vol. 46, No. 8, pp. 1319-1342. Elsevier.

[2] Bourdin, B., Francfort, G. A., and Marigo, J.-J. 2008. The variational approach to fracture, *Journal of Elasticity*, Vol. 91, pp. 5-148. Springer

[3] Ambati, M., Gerasimov, T., and De Lorenzis, L. 2015. A review on phase-field models of brittle fracture and a new fast hybrid formulation, *Computational Mechanics*, Vol. 55, pp. 383-405. Springer.

[4] Feng, D.-C., and Wu, J.-Y. 2018. Phase-field regularized cohesive zone model (CZM) and size effect of concrete, *Engineering Fracture Mechanics*, Vol. 197, pp. 66-79. Elsevier.

[5] Yang, Z.-J., Li, B.-B., and Wu, J.-Y. 2019. X-ray computed tomography images based phase-field modeling of mesoscopic failure in concrete, *Engineering Fracture Mechanics*, Vol. 208, pp. 151-170. Elsevier.

[6] Wu, J.-Y. 2017. A unified phase-field theory for the mechanics of damage and quasi-brittle failure, *Journal of the Mechanics and Physics of Solids*, Vol. 103, pp. 72-99. Elsevier

[7] Griffith, A. A. 1924. Theory of rupture. In Carpinteri et al (eds), *Proceedings of 1st International Congress of Applied Mechanics*; pp. 55-63.

[8] Miehe, C., Welschinger, F., and Hofacker, M. 2010. Thermodynamically consistent phase-field models of fracture: Variational principles and multi-field FE implementations, *International Journal for Numerical Methods in Engineering*, Vol. 83, No. 10, pp. 1273-1311. Wiley Online Library.

[9] Bourdin, B., Francfort, G. A., and Marigo, J.-J. 2000. Numerical experiments in revisited brittle fracture, *Journal of the Mechanics and Physics of Solids*, Vol. 48, No. 4, pp. 797-826. Elsevier.

[10] Nguyen, T.-T., Yvonnet, J., Zhu, Q.-Z., Bornert, M., and Chateau, C. 2016. A phase-field method for computational modeling of interfacial damage interacting with crack propagation in realistic mi-

crostructures obtained by microtomography, *Computer Methods in Applied Mechanics and Engineering*, Vol. 312, pp. 567-595. Elsevier.

[11] Li, W., Nguyen-Thanh, N., and Zhou, K. 2022. Phase-field modeling of interfacial debonding in multi-phase materials via an adaptive isogeometric-meshfree approach, *Engineering Fracture Mechanics*, Vol. 269, p. 108481. Elsevier.

[12] Keerthana, K. 2019. Studies on flexural fatigue behaviour of plain concrete – Mechanisms of crack growth, effect of loading amplitude, frequency, and notch size, *Ph.D. thesis*, Indian Institute of Science.